Journal of the Korean Chemical Society
2015, *Vol. 59, No. 1*
Printed in the Republic of Korea
http://dx.doi.org/10.5012/jkcs.2015.59.1.97

단신 (Notes)

Quantum Dot (QD) Sensitizer on the Surface of TiO_2 Film: Effect of Metal Salt Anions Dissolved in Chemical Bath on the Distribution Density of SILAR-Grown PbS QDs

Hyo Joong Lee[†,‡,*], Yong Lee[†], and Uchirbant Altantuya[†]

[†]*Department of Chemistry, Chonbuk National University, Jeonju 561-756, Korea (ROK)*
[‡]*Department of Bioactive Material Sciences, Chonbuk National University, Jeonju 561-756, Korea (ROK)*
[*]*E-mail: solarlee@jbnu.ac.kr*

(Received September 22, 2014; Accepted December 5, 2014)

Key words: PbS quantum dot, SILAR process, Growth pattern, Quantum dot-sensitized solar cells

INTRODUCTION

Recently, quantum dots (QDs) have attracted much attention for a variety of optoelectronic applications based on their strong light absorption and bright emission over a broad range of spectrum.[1,2] One of the most recent and active areas is related with QD-sensitized solar cells that utilize inorganic QDs as a light harvester.[3,4] QDs are considered as an ideal sensitizer because their absorption range from visible to IR spectrum can be tuned easily by changing the size or composition of QD itself.[5] QDs have also demonstrated a very special characteristic by showing a possibility of two or more exciton generation per one photon absorbed, which is generally termed as multiple exciton generation (MEG).[6] In most studies, QD sensitizers have been prepared by two different methods and incorporated into a variety of structures for photovoltaic devices; *in-situ* chemical bath-deposited QD sensitizers look suitable for mesoporous metal oxide-based photoelectrochemical cells,[7] while *ex-situ* pre-synthesized colloidal QD sensitizers have been applied in very thin film-type solar cells composed of QD/polymer[8] or QD alone[9] between two electrodes. The successive ionic layer adsorption and reaction (SILAR) process is a representative chemical bath deposition technique for preparing target QDs on the surface of mesoporous metal oxide films by dipping the electrode alternatively in cationic or anionic chemical bath. The SILAR can be considered as a sort of ionic layer adsorption process to combine the target cation and anion successively at room temperature.[10] However, there have been few investigations on the detailed experimental conditions of the SILAR process and their effects on the performance of as-prepared QD sensitizers although it has been applied routinely so far in many studies. In this study, it has been observed clearly that the counter-anions (*nitrate* vs. *acetate*) of a metal cation (Pb^{2+}) could play an important role in determining the distribution density of QDs adsorbed during the typical SILAR process for growing PbS QDs on the surface of TiO_2 mesoporous films. In addition, it was successfully demonstrated that the *phase image* obtained with atomic force microscopy (AFM) could be used as a distinguishable map to show the distribution of QDs deposited on the surface of metal oxide at each growth stage, along with a high-resolution transmission electron microscopy (TEM) image. In the design of efficient QD sensitizers over the surface of mesoporous metal oxide, it is very important to get a knowledge of the adsorption pattern and distribution density of QDs and thus determine the experimental conditions for SILAR process for both effective light absorption and efficient charge separation at the interface of metal oxide and QD sensitizers.

EXPERIMENTAL

All chemicals were used as received; $Pb(NO_3)_2$, $Pb(CH_3COO)_2{\cdot}3H_2O$, and Na_2S were purchased from Sigma-Aldrich. The compact TiO_2 layer for AFM imaging experiment was prepared by following a typical spray-pyrolyzed deposition by using a solution of titanium diisopropoxide bis(acetylacetonate) in ethanol.[11] For TEM imaging and absorbance measurements, about 2 μm thickness of TiO_2 mesoporous films were prepared by the doctor-blade technique using a commercial paste (Solaronix; Ti-Nanoxide, T/SP) after dilution. To make a PbS QD-sensitized solar cell, the FTO glass (2.2 mm, 8 Ω/sq.) was pretreated with $TiCl_4$ for 30 min., and then heated to 450 °C to make a thin

blocking TiO_2 layer. Using screen-printing machine and commercial TiO_2 pastes, about 5 μm thick TiO_2 blend layer (Dyesol, 18NR-AO; TiO_2 particle size 20–450 nm) and ~4 μm scattering layer (Dyesol, WER2-O; TiO_2 particle size 150–250 nm) were deposited successively and then sintered to make a mesoporous film. Finally, the typical $TiCl_4$-posttreatment was applied. For growing the PbS QD sensitizer, the SILAR process was done by alternative dipping of as-prepared FTO/TiO_2 films in each aqueous solution of 20 mM $Pb(NO_3)_2$ or $Pb(CH_3COO)_2$ and 20 mM Na_2S. Between dipping, a washing step was included for 1 min in pure DI water. The counter electode was a typical platinized FTO glass. The as-prepared photoanode and counter electrode were combined by hot-press machine through Surlyn film, and the electrolyte solution was injected through a pre-drilled hole through the counter electrode. The electrolyte was composed of 0.2 M Co(O-phenanthroline)$_3$(TFSI)$_2$, 0.05 M Co(O-phenanthroline)$_3$(TFSI)$_3$, 0.1 $LiClO_4$ in acetonitrile. The absorbance was measured by UV-visible spectrometer (S-3100, SCINCO) and TEM was taken by JEM-2200FS (JEOL) instrument. The tapping-mode AFM images were obtained by using Veeco Dimension V. The current-voltage measurements under standard illuminating condition (1 sun) were done using a solar simulator (Peccell, PEC-L01) and a potentiostat (IVIUM, Compactstat).

RESULTS AND DISCUSSION

Two sets of PbS QD from frequently-encountered counter anions (*nitrate* vs. *acetate*) were prepared by a typical SILAR process on the surface of mesoporous TiO_2 film (~2 μm thickness), and their growth was monitored by the naked eye, absorption, and TEM image (*Fig*. 1).

The PbS QD-sensitized electrodes prepared using acetate anions clearly became darker at a faster pace than those from nitrate anions (upper inset of *Figs*. 1a and 1b), under the same experimental conditions except for the counter anion of lead cation dissolved in the chemical bath. Generally, in the reports on the SILAR process for the deposition of QDs, the *solvent* dissolving ions and the *concentration of ions* have been taken into account as an important parameter that affects the growth pattern, but with a limited set of experimental evidences.[12,13] Therefore, the specific experimental conditions reported in previous studies showing a good result have been just adopted in subsequent researches without knowing the exact reasons. In the current study, while investigating the effect of different lead salts on as-grown PbS QDs in a typical SILAR process for efficient QD-sensitized solar cells, the counter anions of the lead cation were found to be a crucial factor in controlling the adsorption density of the metal cation. The amount of Pb cations adsorbed is directly proportional to the amount of PbS QDs formed subsequently after reaction with sulfide anions in each cycle, which could be estimated by the degree of color change in each SILAR cycle. The acetate-induced PbS QDs made a much darker film compared to the nitrate-induced QDs at each cycle of the SILAR process (upper inset of *Figs*. 1a and 1b), which was confirmed by absorbance measurements of the two films (*Figs*. 1a and 1b). For comparison, the magnitude of light-absorption by PbS after the 2nd SILAR cycle in the acetate chemical bath (*Fig*. 1b) is very similar to that after the 5th cycle in the nitrate bath (*Fig*. 1a). To obtain a kind of visual infor-

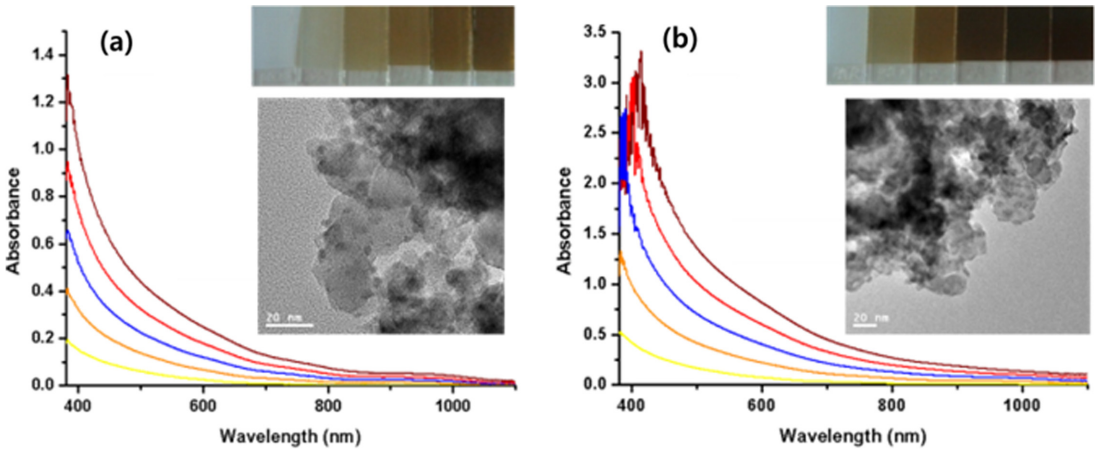

***Figure* 1.** Absorption spectra taken after each SILAR cycle (1~5th) for growing PbS QDs from (a) $Pb(NO_3)_2$ and (b) $Pb(CH_3COO)_2$ bath (inset: HR-TEM images after each 5th cycle and digital pictures of PbS-sensitized TiO_2 film on FTO glass after successive SILAR cycles from 0th to 5th).

mation about the distribution of PbS QDs over TiO_2, high-resolution TEM images were taken after the 5th SILAR deposition from the two films (insets in *Fig.* 1); small particles (PbS) of a few nanometer sizes (3–5 nm) were clearly observed to be distributed much more densely with the acetate-induced PbS than with the nitrate-induced PbS on the surface of larger TiO_2 particles (20–30 nm). Based on the apparent differences in the degree of color change (absorption) and nanoscale distribution of PbS QDs (TEM images), it now appears to be straightforward that the acetate anions induced a much higher density of PbS QD deposition than the nitrate anions did under the same SILAR conditions.

Although a few recent reports on nanometer-resolution imaging of various QD distributions over metal oxide nanoparticles have been somewhat successful by using up-to-date high-resolution TEM instruments,[7,14] this analysis tool is still not considered as easily accessible with acceptable cost. In contrast, atomic force microscopy (AFM) has become a wide-spread tool, and is now considered as a general technique for probing the morphology of a surface with reasonable nanometer-scale resolution, and more convenient accessibility at reasonable costs compared to TEM. However, in the typical topographic imaging of QD sensitizers attached to the surface of a rough metal oxide film, the AFM imaging has not seemed so useful for distinguishing QDs from the supporting metal oxide substrate, and has usually led to blurred images with aggregated particles in reports so far.[15] Therefore, AFM images on QDs/TiO_2 film have been thought of as supporting data by just showing a change of the surface roughness after QD attachment. Nevertheless, a new method (but very classical one in AFM-based studies) has been tried in this study for utilizing AFM as an imaging tool to display the distribution of QDs deposited on TiO_2 film at each growth stage of the SILAR process. For this method, 1) the top surface of mesoporous TiO_2 film was replaced with a compact TiO_2 film as the substrate for AFM imaging, which could provide a similar supporting layer with much less roughness. 2) The phase image was taken rather than the typical topographic image due to its quite superior sensitivity.[16] When a typical AFM-imaging experiment was carried out on the surface of compact TiO_2 film after 1 SILAR process for depositing PbS QDs from $Pb(NO_3)_2$-Na_2S chemical baths, two different mode-based images could be obtained simultaneously, as shown in *Fig.* 2. In the topographic image (*Fig.* 2a), it seems that there are only the typical round-shaped TiO_2 grains with size of about 150 nm, but without any smaller particles (QDs) discriminated. This kind of image is exactly what has been observed so far from QDs on the nano-particulated TiO_2 films, which leads to a conclusion that AFM is not suitable for distinguishing smaller particles from TiO_2-particulated films. However, in the phase image scanned over the same area as that in the topographic one, a distribution of smaller particles or their aggregates is clearly seen as white spots over the flattened grains of TiO_2, because a more sensitive signal of the phase difference rather than an amplitude signal is detected and recorded when the tip is scanned over spots with different chemical compositions. This very sensitive and unique character of phase-difference detection in AFM operation has also been used under the name of *Chemical Force Microscopy* (CFM) for distinguishing different materials mixed at the nanometer scale.[17] In the phase image of *Fig.* 2b, two different materials, PbS and TiO_2, interact with the tapping AFM tip with different magnitudes, thus resulting in a clear change in the phase of the oscillating tip. After one SILAR cycle for growing PbS QDs over the surface of TiO_2 film, a random distribution of PbS seeds was imaged with a higher density in the region of grain boundaries. From the cross-sectional lines shown below the two images, it looks very clear that the topographic scan cannot differentiate a few to a few tens of nanoparticles from a rather rough surface, while they were detected easily in the phase-mode image. Therefore, this phase image of QDs on the surface of TiO_2 film can be utilized together with high-resolution TEM images for investigating the distributions of QDs at each growth stage, although the TEM images could give a more accurate and absolute size of the QDs. In many related studies, it has been very important to obtain information about the two-dimensional distribution of QDs or nanoparticles over the surface of a substrate.

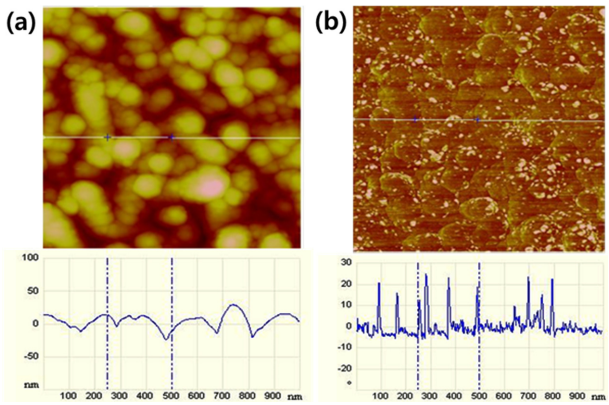

***Figure* 2.** AFM topography (a) and phase (b) images with cross-sectional lines of compact TiO_2 film on FTO glass after 1st SILAR cycle for growing PbS QDs from $Pb(NO_3)_2$ and Na_2S baths.

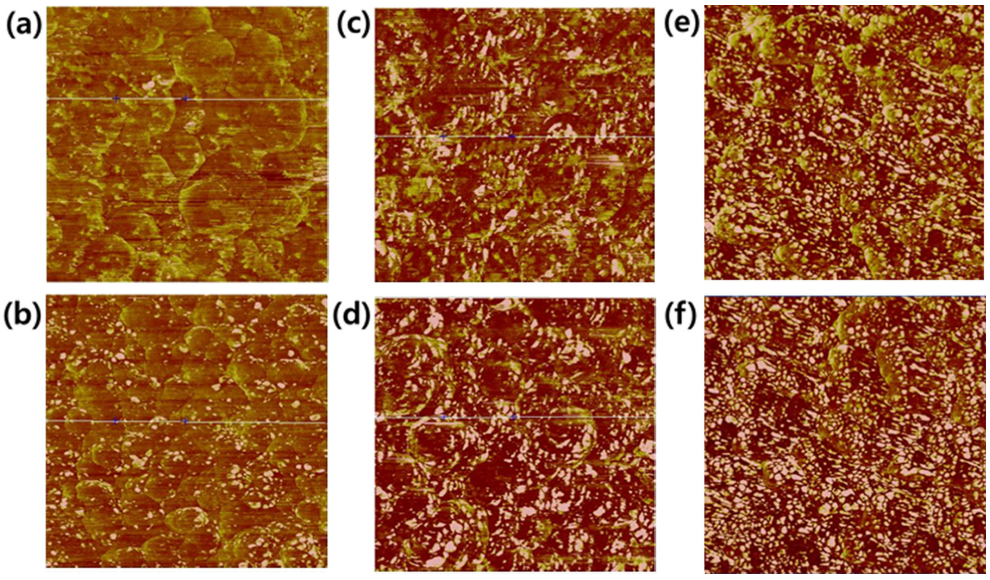

***Figure* 3.** AFM phase images of SILAR-grown PbS QDs on compact TiO_2 film/FTO glass after 1st (b), 3rd (c) and 5th (d) cycles from $Pb(NO_3)_2$-bath while 3rd (e) and 5th (f) from $Pb(CH_3COO)_2$-bath. For reference, (a) was from a bare compact TiO_2 film. Scanned area is 1 μm×1 μm.

To follow up the successive changes in the distribution density of PbS QDs after each SILAR cycle, and to compare the as-obtained results from the two different chemical baths (*lead nitrate* vs. *lead acetate*), two representative phase images after the 3rd and 5th SILAR cycles in each chemical bath were obtained, as shown in *Fig*. 3. As the number of SILAR cycles increased, more bright spots are spread and overlapped in both cases, but with different densities. In the case of the nitrate-induced deposition of PbS QDs (*Figs*. 3 b–d), PbS spots seem to be expanded gradually from the 1st through the 3rd cycle, all the way to the 5th cycle. More numerous and larger bright spots (PbS QDs) are spreading through the surface of the TiO_2 film. When the anion was changed from nitrate to acetate in the chemical bath, a much denser distribution of bright spots was observed in the corresponding phase images (*Figs*. 3 e and f). This different density of the PbS QD deposition in the AFM phase image is consistent with the results obtained from absorbance and TEM images (*Fig*. 1) with the two chemical baths. Overall, the acetate-countered lead cations, later leading to PbS after reaction with sulfide anions, seem to have been adsorbed much more densely and homogeneously than when nitrate was used. This notable difference in the adsorption behavior can be explained by the role of acetate anions in the chemical bath for the SILAR process. The dissolved acetate anion (weak base) raised the pH (~6.5) in the solution (~5.2 in deionized water), into which the TiO_2 film is dipped. Then, the TiO_2 surface can be negatively charged due to a higher value of pH (~6.5) than the point of zero charge (pzc) of TiO_2 (~5.5),[18,19] and accordingly, could attract Pb^{2+} cations more strongly than the positively-charged surface at the lower pH (~4.0) induced by nitrate anions. Secondly, acetate anions can be adsorbed on the TiO_2 surface via carboxylate group, which is a typical linker in molecular dyes in dye-sensitized solar cells. Therefore, the more negatively charged surface of TiO_2 could attract more Pb^{2+} cations in the SILAR process, finally leading to a denser PbS on the surface of TiO_2. The same situation was observed when cadmium ions (Cd^{2+}) were used instead of Pb^{2+}. A similar behavior in the case of PbS/CdS QD deposition was observed and reported recently.[20] More studies including other metal cations and anions are in progress for clarifying the mechanism and reaching a general conclusion for the SILAR-based chemical bath deposition of QDs.

In most of QD-sensitized solar cells, the size of the QD sensitizer is very critical in terms of light absorption and electron injection into the conduction band (CB) of the metal oxide.[21] The size of the QDs deposited in the SILAR process is increased gradually after each cycle. Therefore, it is necessary to examine the optimal number of SILAR cycles in preparing the target QD sensitizer for maximizing the photon-to-current conversion efficiency. In previous studies,[22–25] a few SILAR cycles (3 to 6) were observed to be enough to make proper PbS QDs with favorable band positions for effective charge transfers, while the number

***Table* 1.** SILAR-grown PbS QD sensitizer-based phototovoltaic data from two different chemical baths (lead nitrate and lead acetate)

Lead precursor/# of SILAR cycle	J_{sc} (mA/cm^2)	V_{oc} (V)	Fill factor (FF)	Conversion Efficiency (η, %)
$Pb(NO_3)_2$-3	2.01	0.36	0.55	0.40
$Pb(NO_3)_2$-4	2.29	0.39	0.55	0.49
$Pb(NO_3)_2$-5	3.82	0.39	0.55	0.82
$Pb(Ac)_2$-2	2.34	0.40	0.54	0.51
$Pb(Ac)_2$-3	2.29	0.41	0.50	0.47
$Pb(Ac)_2$-4	1.90	0.39	0.50	0.37

of cycles seemed unlimited (if the mesopores in the film were not blocked) in the deposition of CdS due to the favorable band position of its bulk state relative to that of TiO_2. The band position of PbS QDs is very sensitive to the size, and thus, to the number of SILAR cycles.[14,23] As expected, the nitrate-induced PbS QD sensitizer showed a different pattern of change in the photovoltaic performance compared with the acetate-induced PbS counterpart, in that the efficiency of the nitrate-induced sensitizer in a typical configuration of QD-sensitized solar cells was increased up to the 5th SILAR cycle, and then decreased, while that of the acetate-induced sensitizer was decreased gradually from the 3rd cycle, as summarized in *Table* 1. Although the absolute values of overall power conversion efficiency are relatively low from the usage of less efficient cobalt(II/III) redox couple rather than polysulfide electrolyte due to its incompatibility, those photovoltaic results are also consistent with the different distributions observed in *Figs*. 1–3. In the case of nitrate, the initial deposition of PbS was observed to be quite scattered, and then PbS was grown gradually and overlapped slowly. Therefore, the best results were obtained at around the 5th cycle of the SILAR process. In contrast, the acetate induced too much deposition of the PbS in the initial stages due to strong interactions, and the PbS reached a critical point around 2 cycles for effective charge injection. From the 3rd cycle, the injection efficiency may be decreased due to the overgrown or overlapped state of PbS QDs.

CONCLUSION

The counter-anion of the lead cation used in the SILAR process for an ionic layer-by-layer deposition of target PbS QDs was observed to exert a notable influence on the adsorption density of cations and the consequent QDs grown on the surface of metal oxides. As a new detection tool, AFM phase imaging was successfully demonstrated to distinguish the deposited QDs from the metal oxide substrate, and is considered to be very effective when used together with absorbance and high-resolution TEM images. With these valuable findings about the distribution density and its change of SILAR-grown QDs, researchers will be able to design either material- or purpose-specific experimental conditions for preparing efficient QDs on the surface of various metal oxide substrates.

Acknowledgments. H. J. Lee acknowledges the financial support by the National Research Foundation (no. 2012R1A1A1015528). H. J. Lee is also greatly appreciated for the help given by the late Prof. S.-M. Park in carrying out AFM and TEM experiments, and by Ms. Ji-Young Oh in obtaining the photograph of PbS-SILAR processed TiO_2-films.

REFERENCES

1. Murray, C. B.; Norris, D. J.; Bawendi, M. G. *J. Am. Chem. Soc.* **1993**, *115*, 8706.
2. Bera, D.; Qian, L.; Tseng, T.-K.; Holloway, P. H. *Materials* **2010**, *3*, 2260.
3. Kamat, P. V. *J. Phys. Chem. Lett.* **2013**, *4*, 908.
4. Kamat, P. V. *Acc. Chem. Res.* **2012**, *45*, 1906.
5. Hines, M. A.; Scholes, G. D. *Adv. Mater.* **2003**, *15*, 1844.
6. Beard, M. C.; Luther, J. M.; Semonin, O. E.; Nozik, A. J. *Acc. Chem. Res.* **2013**, *46*, 1252.
7. Lee, H.; Wang, M.; Chen, P.; Gamelin, D. R.; Zakeeruddin, S. M.; Grätzel, M.; Nazeeruddin, Md. K. *Nano Lett.* **2009**, *9*, 4221.
8. Xu, T.; Qiao, Q. *Energy Environ. Sci.* **2011**, *4*, 2700.
9. Kramer, I. J.; Sargent, E. H. *ACS Nano* **2011**, *5*, 8506.
10. Lee, H. J.; Bang, J.; Park, J.; Kim, S.; Park, S.-M. *Chem. Mater.* **2010**, *22*, 5636.
11. Lee, H. J.; Yum, J.-H.; Leventis, H. C.; Zakeeruddin, S. M.; Haque, S. A.; Chen, P.; Seok, S. I.; Grätzel, M.; Nazeeruddin, Md. K. *J. Phys. Chem. C* **2008**, *112*, 11600.
12. Chang, C.-H.; Lee, Y.-L. *Appl. Phys. Lett.* **2007**, *91*, 053503.
13. Hossain, M. A.; Jennings, J. R.; Shen, C.; Pan, J. H.; Koh, Z. Y.; Mathews, N.; Wang, Q. *J. Mater. Chem.* **2012**, *22*, 16235.
14. Lee, J.-W.; Son, D.-Y.; Ahn, T. K.; Shin, H.-W.; Kim, I. Y.; Hwang, S.-J.; Ko, M. J.; Sul, S.; Han, H.; Park, N.-G. *Sci. Rep.* **2013**, *3*, 1050.
15. Lee, Y.-L.; Lo, Y.-S. *Adv. Func. Mater.* **2009**, *19*, 604.
16. http://afmhelp.com/index.php?option=com_content&view=article&id=84:what-is-phase-imaging.
17. Vezenov, D. V.; Noy, A.; Ashby, P. *J. Adh. Sci. Tech.* **2005**, *19*, 313.
18. Jin, H.; Choi, S.; Velu, R.; Kim, S.; Lee, H. J. *Langmuir* **2012**, *28*, 5417.
19. Palomares, E.; Clifford, J. N.; Haque, S. A.; Lutz, T.; Durrant, J. R. *J. Am. Chem. Soc.* **2003**, *125*, 475.
20. Gonzalez-Pedro, V.; Sima, C.; Marzari, G.; Boix, P. P.;

Gimenez, S.; Shen, Q.; Dittrich, T.; Mora-Sero, I. *Phys. Chem. Chem. Phys.* **2013**, *15*, 13835.
21. Kamat, P. V. *J. Phys. Chem. C.* **2008**, *112*, 18737.
22. Robel, I.; Kuno, M.; Kamat, P. V. *J. Am. Chem. Soc.* **2007**, *129*, 4136.
23. Braga, A.; Gimenez, S.; Concina, I.; Vomiero, A.; Mora-Sero, I. *J. Phys. Chem. Lett.* **2011**, *2*, 454.
24. Lee, H.; Leventis, H. C.; Moon, S.-J.; Chen, P.; Ito, S.; Haque, S. A.; Torres, T.; Nüesch, F.; Geiger, T.; Zakeeruddin, S. M.; Grätzel, M.; Nazeeruddin, Md. K. *Adv. Func. Mater.* **2009**, *19*, 2735.
25. Lee, H. J.; Chen, P.; Moon, S.-J.; Sauvage, F.; Sivula, K.; Bessho, T.; Gamelin, D. R.; Comte, P.; Zakeeruddin, S. M.; Seok, S. I.; Grätzel, M.; Nazeeruddin, Md. K. *Langmuir* **2009**, *25*, 7602.
26. Plass, R.; Pelet, S.; Krueger, J.; Grätzel, M.; Bach, U. *J. Phys. Chem. B* **2002**, *106*, 7578.